Environmental Pollution 246 (2019) 668–677

Contents lists available at ScienceDirect

Environmental Pollution

journal homepage: www.elsevier.com/locate/envpol

Seasonal variation of chemical characteristics of fine particulate matter at a high-elevation subtropical forest in East Asia☆

Celine S.L. Lee [a], C.C.-K. Chou [a, *], H.C. Cheung [a], C.-Y. Tsai [a], W.-R. Huang [a], S.-H. Huang [a], M.-J. Chen [a], H.-T. Liao [b], C.-F. Wu [c], T.-M. Tsao [d], M.-J. Tsai [d], T.-C. Su [e]

[a] Research Center for Environmental Changes, Academia Sinica, Taipei, Taiwan
[b] Institute of Occupational Medicine and Industrial Hygiene, National Taiwan University, Taipei, Taiwan
[c] Department of Public Health, National Taiwan University, Taipei, Taiwan
[d] School of Forestry and Resource Conservation, National Taiwan University, Taipei, Taiwan
[e] Department of Internal Medicine and Cardiovascular Center, National Taiwan University Hospital, Taipei, Taiwan

ARTICLE INFO

Article history:
Received 23 May 2018
Received in revised form
1 October 2018
Accepted 11 November 2018
Available online 23 November 2018

Keywords:
$PM_{2.5}$
Urban air pollution
Mountain-valley circulations
Subtropical forest
Sulfur oxidation ratio
Nitrogen oxidation ratio

ABSTRACT

The aim of this study was to chemically characterize the fine particulate matter ($PM_{2.5}$) at a subtropical forest in East Asia under the influences of anthropogenic and biogenic sources and a complex topographic setting. Four seasonal campaigns were conducted at the Xitou Experimental Forest in central Taiwan from the winter of 2013 to the autumn of 2014. The results indicated that the ambient levels and chemical features of $PM_{2.5}$ exhibited pronounced seasonal variations. Non-sea-salt sulfate (nss-SO_4^{2-}) constituted the major component of $PM_{2.5}$, followed by ammonium (NH_4^+) and nitrate (NO_3^-) during winter, summer and autumn. However, it was revealed that the mass fraction of NO_3^- increased to be comparable with that of nss-SO_4^{2-} in springtime. The mass contribution of secondary organic carbon (SOC) to $PM_{2.5}$ peaked in summer (13.2%), inferring the importance of enhanced photo-oxidation reactions in SOC formation. Diurnal variations of O_3 and SO_2 coincided with each other, suggesting the transport of aged pollutants from distant sources, whereas CO and NO_x were shown to be under the influences of both local and regional sources. Notably high sulfur oxidation ratio (SOR) and nitrogen oxidation ratio (NOR) were observed, which were 0.93 ± 0.05 and 0.39 ± 0.20, respectively. Precursor gases (i.e. SO_2 and NO_x) could be converted to sulfate and nitrate during the transport by the uphill winds. Furthermore, due to the high relative humidity at Xitou, enhanced aqueous-phase and/or heterogeneous reactions could further contribute to the formation of sulfate and nitrate at the site. This study demonstrated the significant transport of urban pollutants to a subtropical forest by the mountain-valley circulations as well as the long-range transport from regional sources, whereas the implications of which for regional climate change necessitated further investigation.

© 2018 Elsevier Ltd. All rights reserved.

1. Introduction

Aerosols can directly affect the Earth's radiation balance by absorbing and scattering solar radiation and indirectly by altering cloud properties and lifetimes (Charlson et al., 1992; Myhre, 2009), and have severe adverse impact on human health (Anderson et al., 2012; Kim et al., 2015a; Lelieveld et al., 2015). The study of physiochemical properties of aerosols are of vital importance to evaluate the impacts on climate and human health.

To date, there is still large uncertainty associated with aerosol radiative forcing in climate models (Solomon et al., 2007; Seinfeld and Pandis, 2006), primarily due to the complex nature of ambient aerosols with different physical and chemical properties, whereas the concentration and composition of aerosols vary on different temporal and spatial scales (Tsigaridis et al., 2014; Ma and Yu, 2015; Kim et al., 2015b). The nature of the sources (i.e. natural and anthropogenic sources), the atmospheric physical and/or chemical processes, and the interactions between meteorological and atmospheric chemistry features are major factors influencing these variations. The complexity of factors affecting the large variations observed in aerosol properties are especially pronounced in East Asia, where particulate matter and their precursors from

☆ This paper has been recommended for acceptance by Dr. Kimberly Hageman.
* Corresponding author.
E-mail address: ckchou@rcec.sinica.edu.tw (C.C.-K. Chou).

https://doi.org/10.1016/j.envpol.2018.11.033
0269-7491/© 2018 Elsevier Ltd. All rights reserved.

various sources are emitted in large quantities and have caused severe deterioration to regional air quality (Lee et al., 2005; Yuan et al., 2006; Chang et al., 2010; Chou et al., 2010, 2017; Li et al., 2016). Taiwan is located within the East Asia region, where many cities (including a few with over 2 million inhabitants) were built on the western side of the Central Mountain Range, which is covered with forested areas and more than 25 summits exceeding 3000 m above sea level (a.s.l.). These unique environmental features provide an ideal setting to study impact of anthropogenic sources on a forest environment, which could provide further insights to atmospheric processing of anthropogenic and biogenic emissions. Moreover, the complex topography of the island induces orographic lifting, which could interact with land-sea breeze circulations and large-scale monsoon systems in the western plain of Taiwan (Lin et al., 2008; Kerns and Chen, 2010). A number of intensive short-term studies have been conducted on physiochemical properties of aerosols and their components at high-elevation forest sites in East Asia, such as those in southern China (Li et al., 2010; Gao et al., 2012; Zhou et al., 2012), Japan (Kido et al., 2001a, 2001b) and Taiwan (Lee et al., 2011; Chuang et al., 2014). Although many studies have been conducted in East Asia, particularly in northern and eastern China region, on the impacts of haze pollution in urban environments over the past decade (Sun et al., 2006; Cao et al., 2012; Sun et al., 2013; Tian et al., 2016), relatively few studies have been initiated to examine impact of severe anthropogenic pollution on a forest environment and information on seasonal variations of aerosol and its chemical composition for a high-elevation forest environment in this region is still limited.

To further investigate the characteristics of seasonal variation of aerosols under the impacts of anthropogenic sources on a subtropical forest, we conducted four seasonal measurement campaigns of $PM_{2.5}$ (particulate matter with aerodynamic diameters less than 2.5 μm) at Xitou, Taiwan. The present study aimed to characterize concentration and chemical composition of aerosols in different seasons, and elucidate controlling factors for the seasonal patterns. The results are useful to unravel the complex mechanisms of chemical processes involved in the formation of secondary aerosols, and to formulate parameterization of atmospheric aerosol processes for climate and air quality models.

2. Methodology

2.1. Observation site

Four seasonal measurement campaigns were conducted in Xitou Experimental Forest of National Taiwan University (23.6°N, 120.8°E) from winter of 2013 to autumn of 2014. Fig. 1 shows the geographical location of Xitou forest. The forest is located in Nantou County of Taiwan, which is approximately 1120 m a.s.l. (above sea level) with an area of 2500 ha, comprised primarily of cypress and ginkgo trees. Xitou forest is located at a high-elevated section of a valley, on the western slope of the Central Mountain Range (Fig. 1). It is surrounded by mountainous terrain on the three sides, bounded by the Fenghuang Mountain Range in the east, Lingtou Mountain (2025 m a.s.l.) and its extension in the south and west. The site has been known to be affected by a regular daily wind pattern, with northern valley winds during daytime and southerly mountain winds during nighttime (Simon et al., 2016). A metropolis of Taichung (with around 3 million inhabitants; at 90 m a.s.l.) is located at about 50 km to the northwest of Xitou (Fig. 1), which is a large urban environment comprising of residential and industrial premises including mainly electronic and semi-conductors, precision machinery, metallic, plastic and chemical products (Taichung Science Park and Taichung Industrial Park website, assessed in September 2018) and it is where the largest coal-fired power plant is located. Changhua and Yunlin County are adjacent to Nantou County (in which Xitou Forest is located), which contain a wide area of agricultural lands as well as industrial areas, comprising of textiles, plumbing equipment, bicycles and flower industries in Changhua and livestock and fishery farming, and petrochemical products (from Mailiao Industrial Complex) in Yunlin (Changhua and Yunlin County government website and Ministry of Economics, Taiwan website, assessed in September 2018). The area of central Taiwan has been known to be affected by severe pollution from sources such as power plant coal combustion, traffic, oil burning, oil combustion, and industrial sources (such as Iron ore and steel industries) (Cheng et al., 2009; Chen et al., 2015; Hsu et al., 2017).

2.2. Meteorological conditions

During the study period, the average temperature was 14.9, 15.2, 20.7 and 19.0 °C, and the average relative humidity was 87.1, 92.1, 91.4 and 91.4%, for winter, spring, summer and autumn, respectively. The wind patterns during the four seasons are mainly dominated by northwesterly and southeasterly winds (Fig. S1 in the Supplementary material) arising from the mountain-valley circulation.

2.3. Instrumentation

In this study, a total of 88 sets of $PM_{2.5}$ filter samples were collected from 09:00 to 07:00 (LT) of the next day. The sampler was located in an open area within the forest and sampling flow rate was set to 6.7 L/min for each channel. Leakage check and flow calibrations were conducted daily. Further details on aerosol sampling, gaseous and meteorological measurement can be found in S1 of the Supplementary material, and the methodology is briefly described here. The filter samples were analyzed for water-soluble ions via ion chromatograpy (Dionex ICS 1000, Thermo Scientific). Organic carbon (OC) and elemental carbon (EC) were measured by a thermal/optical carbon analyzer (DRI, 2001A, Atmoslytic Inc.), following the IMPROVE thermo-optical reflectance (TOR) protocol (Chow et al., 2001). Crustal elements and metals contained in $PM_{2.5}$ samples, including Fe, Mn, Cr, Ni, Pb, Si, Ti, V and Zn, were measured using energy dispersive X-ray fluorescence (ED-XRF) (Epsilon 5, PANalytical) (RTI, 2009). Hourly $PM_{2.5}$ concentration was measured using a Tapered Element Oscillating Microbalance (TEOM) (1405DF, Thermo Electron). O_3 was measured by a UV photometry instrument (49i, Thermo Scientific) and SO_2 was measured by a pulsed UV fluorescence analyzer (43i-TLE, Thermo Electron). NO_x was detected with a chemiluminescence analyzer (CLD 88p, Eco Physics) and a photolytic converter (PLC 860, Eco Physics). CO was measured with a gas filter correlation infrared analyzer (48i-TLE, Thermo Electron). Meteorological parameters, including wind speed (WS) and direction (WD), temperature and relative humidity (RH) were acquired from a meteorological station located at the same location as our site and maintained by the National Taiwan University. The details of the data processing can be found in S2 of the Supplementary material.

3. Results and discussion

3.1. Aerosol concentration and composition overview

Table 1 provides a summary of descriptive statistics in terms of seasonal mean and annual mean of mass concentrations of $PM_{2.5}$ and its constituents. The mean concentrations of $PM_{2.5}$ measured in this study were 19.1, 26.3, 11.5 and 21.3 μg/m^3 for winter, spring, summer and autumn, respectively, and the total average was 18.7 μg/m^3, which was lower than that measured in urban and

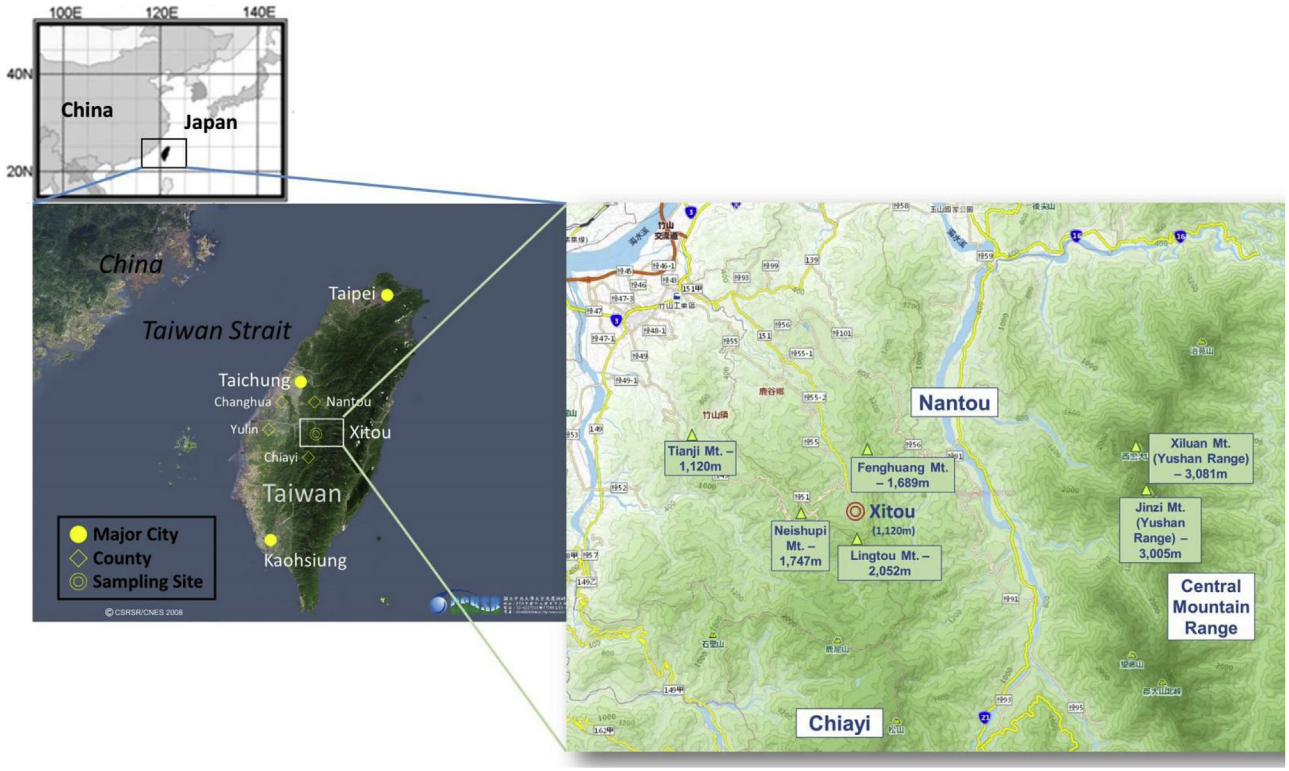

Fig. 1. Geographic locations of Taiwan in East Asia and Xitou on the Taiwan Island (with a topographic overview around Xitou).

suburban areas in Taichung city, and Yunlin and Changhua County (Kuo et al., 2013; Hsu et al., 2017). In comparison with other high-elevation sites worldwide, the mass concentrations of $PM_{2.5}$ and inorganic species at Xitou were generally higher than the levels in San Gorgonio and Great Smoky Mountain in southern U.S. (Lee et al., 2008), but lower than those measured in Mount Tai, northern China (Zhou et al., 2010). The mass concentrations of $PM_{2.5}$ and carbonaceous species were comparable to those in Mount Lu and Mount Heng, southern China (Zhou et al., 2012; Li et al., 2015), but lower than those in Nagarkot, Nepal (Carrico et al., 2003) in southern Asia which is under the influences of dense regional haze (Lelieveld et al., 2001; Collins et al., 2002; Venkataraman et al., 2002; Satake et al., 2004; Rengarajan et al., 2007). The details of the comparisons can be found in S3 of the Supplementary material.

Fig. 2 depicts an overview of seasonally averaged chemical compositions of $PM_{2.5}$. Non-sea-salt sulfate was found to be the major constituent of $PM_{2.5}$, followed by NH_4^+ and then NO_3^- in $PM_{2.5}$ during winter, summer and autumn. It is noteworthy that high fraction of NO_3^- (23.5%) was observed in spring which contributed comparably with the nss-SO_4^{2-} (23.2%) to the $PM_{2.5}$ mass. A possible reason to this is the release of nitrogen oxides due to fertilization in springtime at high-elevated tea plantations surrounding Xitou site and farmlands (e.g. ricefields and fruit plantations) in adjacent counties, such as Changhua and Yulin (see Fig. 1). The primary organic carbon (POC) fraction was slightly higher in winter and spring than that in summer and autumn. A notably high fraction of secondary organic carbon (SOC) was found in summertime (13.2%), whereas lower mass fraction of SOC was found during colder seasons. The EC fraction was similar during winter, spring and summer (4.6–4.7%), although a lower fraction was found during autumn (3.6%). The NH_4^+ fraction was found to be similar during winter, spring and summer seasons (12.3–13.8%), and autumn was found to have the highest fraction of NH_4^+ (19.9%), although there is no clear explanation to this yet. The dust and sea-salt fractions contributed to relatively smaller fractions in $PM_{2.5}$, showing that the influences from crustal materials and sea-salts were minimum.

3.2. Diurnal variations

Fig. 3a–d shows diurnal profiles of $PM_{2.5}$ (from TEOM measurement), SO_2, NO_x, O_3 and CO as well as meteorological parameters at Xitou, which is a highly elevated site surrounded by mountains in all sides, except in the northwest direction (Fig. 1), and this topographical feature has affected the transport of pollutants to the site. $PM_{2.5}$ and all the gaseous pollutants exhibited diurnal patterns with higher concentrations during daytime and lower concentrations at nighttime. All pollutants, including $PM_{2.5}$, SO_2, NO_x, O_3 and CO, increased sharply around 7:00–9:00 LT and peaked around 14:00–16:00 LT, which coincide with the increase in temperature accompanied by a change in wind direction to the northwesterly winds; and they decreased significantly around 16:00–18:00 LT with the decrease in temperature and change in wind direction to southeasterly winds (see Fig. 3a–d). This could attribute to onset of surface heating in the morning and differential heating between bottom of the valley and the mountain ridge, causing vertical transport of pollutants along with the uplifting of planetary boundary layer (PBL) (see Fig. S8 and Section S8). SO_2, O_3 and $PM_{2.5}$ were found to decrease at earlier time than NO_x and CO, which is most explicitly shown in the diurnal trend during winter and autumn (Fig. 3a and d). Although traffic could emit primary pollutants, including NO_x, CO and $PM_{2.5}$, secondary pollutants such as O_3 and $PM_{2.5}$ were likely formed and transported along the precursor gases (e.g. SO_2) from emission sources such as coal-combustion power plant, municipal waste incinerator, and industrial sources in downhill areas by the northwesterly winds, and the pollutant concentrations decreased while the southeasterly winds prevailed bringing cleaner air mass from the higher mountain ridges (Central mountain range, up to 3000 m) in the southeast

Table 1
Descriptive statistics on mean concentrations of $PM_{2.5}$, major ions and carbonaceous species (in μg/m^3), and crustal elements and metals (in ng/m^3) during the measurement period.

		$PM_{2.5}$	Ca^{2+}	Mg^{2+}	Na^+	NH_4^+	K^+	nss-SO_4^{2-}	NO_3^-	Cl^-	EC	OC	POC	SOC	Fe	Mn	Cr	Ni	Pb	Si	Ti	V	Zn
Winter [b]	Average	19.1	0.05	0.01	0.08	2.56	0.43	6.06	2.16	0.13	0.88	3.49	2.31	1.30	39.4	4.26	4.35	1.05	12.2	73.6	2.41	0.63	23.9
n = 19	σ	11.0	0.02	0.005	0.04	1.45	0.27	3.83	1.43	0.08	0.51	1.84	1.52	0.68	20.6	3.43	1.40	0.20	8.65	54.8	1.12	0.51	17.9
Spring [c]	Average	26.3	0.07	0.02	0.07	3.62	0.61	6.11	6.19	0.39	1.23	4.22	3.28	1.05	42.5	2.47	5.87	1.52	6.83	52.9	2.51	0.90	13.5
n = 22	σ	10.8	0.03	0.01	0.03	1.65	0.29	3.25	3.32	0.28	0.47	1.69	1.43	0.86	33.2	0.90	5.22	1.55	1.76	29.7	1.19	0.58	8.31
Summer [d]	Average	11.5	0.06	0.02	0.09	1.41	0.15	3.01	0.48	0.08	0.53	2.56	1.25	1.52	24.6	1.91	4.42	1.13	5.67	38.2	2.00	0.91	6.45
n = 28	σ	6.31	0.03	0.01	0.05	0.90	0.08	1.81	0.37	0.03	0.31	1.51	0.89	0.88	10.9	0.32	2.51	0.44	1.23	13.0	0.74	0.77	5.06
Autumn [e]	Average	21.3	0.09	0.03	0.12	4.25	0.19	8.68	1.97	0.14	0.77	3.36	2.11	1.56	[a]	[a]	[a]	[a]	[a]	[a]	[a]	[a]	[a]
n = 19	σ	8.09	0.06	0.03	0.08	2.32	0.08	4.48	1.03	0.06	0.53	1.37	1.55	0.57									
Total	Average	18.7	0.07	0.02	0.09	2.82	0.33	5.67	2.59	0.18	0.83	3.35	2.21	1.36	34.8	2.75	4.89	1.24	7.86	53.0	2.29	0.83	13.7
n = 88	σ	10.6	0.04	0.01	0.05	1.93	0.28	3.88	2.86	0.19	0.52	1.70	1.52	0.79	24.2	2.09	3.51	0.96	5.32	36.9	1.03	0.65	12.9

[a] "–" denotes that data is not available.
[b] Winter campaign is from 22 December 2013–10 January 2014; Data is not available on 9 January 2014.
[c] Spring campaign is from 3–24 March 2014.
[d] Summer campaign is from 11 June – 14 July 2014; Data is not available from 14–19 July 2014.
[e] Autumn campaign is from 16 September – 6 October 2014.

region (see Fig. 1). This is different to the diurnal variation of CO and NO_x observed in typical urban site in Taiwan, which peaked during morning and afternoon rush hours (8:00 and 20:00 L.T.) (Chou et al., 2007). The plots of diurnal profiles of $PM_{2.5}$, SO_2, NO_x and O_3 during weekdays and weekends (including public holiday) are also presented in Supplementary material (Figs. S3a-h). Although larger variations were observed in plots of diurnal profiles during weekends/public holidays (as smaller number of days were included in the averaging), there were no significant differences between diurnal trends during weekdays and weekends/public holidays (Figs. S3a–h), which illustrate the increase in pollutant concentrations due to effective transport of pollutants by the mountain-valley circulations.

3.3. Temporal variation of $PM_{2.5}$ and its chemical species

To further investigate the seasonal variations in chemical composition and aerosol characteristics, mass concentrations of $PM_{2.5}$, nss-SO_4^{2-}, NO_3^- and NH_4^+ are plotted in Fig. 4a–d. The meteorological conditions including temperature, relative humidity, wind speed and wind direction are also included in the figures to study their influences on the aerosol concentrations and compositions. The temporal variation of potassium ion (K^+), an important tracer for biomass burning (Andreae, 1983; Dan et al., 2004), is also presented along with OC and EC in Fig. 4a–d. Sulfur dioxide and NO_x are precursor gases and they are plotted against the nss-SO_4^{2-} and NO_3^- in Fig. 4a–d. An overall trend showing the temporal variation of $PM_{2.5}$ and its constituents over the sampling period is depicted in Fig. S4.

A distinct pattern with the northwesterly wind prevailed during daytime and southeasterly wind prevailed during nighttime was generally observed in all seasons, although the wind direction is more mixed during the spring and summer (see Fig. 4a–d and Fig. S1 of the Supplementary material). The episode days are defined as measurement days with a significant simultaneous increment of $PM_{2.5}$ as well as the major components of $PM_{2.5}$, including nss-SO_4^{2-}, NO_3^-, NH_4^+, OC and EC, which are depicted as the peaks in the temporal trends, i.e., peaks as shown in Fig. 4a–d. The increase of pollutants was found to be highly associated with this wind pattern. Given a stable wind pattern (in northwesterly–southeasterly direction), the northwesterly wind can transport the pollutants effectively to the site. This is elucidated, for an instance, by the high episode days during on 28 Dec (EP1) and 5 Jan (EP2) in winter and on 28 Sep (EP6) in autumn when the wind exhibited a distinct diurnal pattern and high concentrations of $PM_{2.5}$, nss-SO_4^{2-}, NO_3^-, NH_4^+, OC and EC were observed, compared to the lower pollutant concentrations on 2 Jan and 22 Sep, when a more mixed wind pattern was observed. The main constituents of $PM_{2.5}$, major ions (nss-SO_4^{2-}, NO_3^-, NH_4^+) and carbonaceous species are shown to be in phase with $PM_{2.5}$ during all seasons. Interestingly, water soluble K^+ concentration was found to change simultaneously with $PM_{2.5}$, and OC and EC concentrations. SO_2 generally varied in phase with nss-SO_4^{2-} in all seasons, while no similar trend was observed between NO_x and NO_3^-. A possible explanation to this could be the effective formation of nss-SO_4^{2-} primarily from SO_2 during the uphill transport (infact it was shown that notably high SOR was found at the site). The formation of NO_3^- could be partly from neutralization of NO_x gases, however, it could be attributed to other sources of NO_3^-, such as from fertilizers (e.g. $Ca(NO_3)_2$) and organonitrates (Perring et al., 2009; Day et al., 2010). SOC was also found to vary closely with $PM_{2.5}$ and carbonaceous species (OC and EC) in all seasons, when the highest OC and elevated SOC concentrations (2.35 μg/m^3; third highest) was observed on 6 July which coincided with the highest temperature recorded in summer (27.9 °C), evidencing strong enhancement of

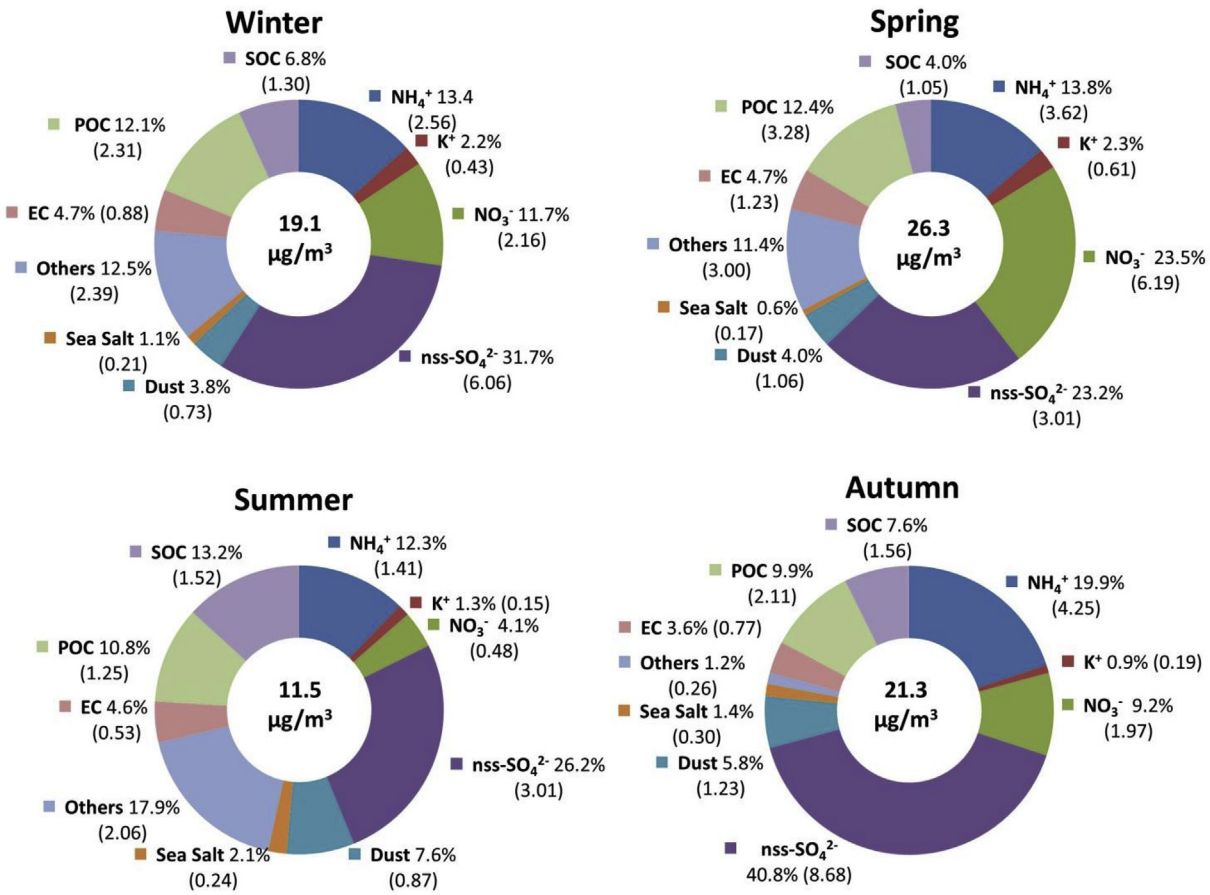

Fig. 2. Averaged compositions of $PM_{2.5}$ for the winter, spring, summer and autumn campaigns of this study. The values in the brackets denote absolute concentrations (μg/m^3).

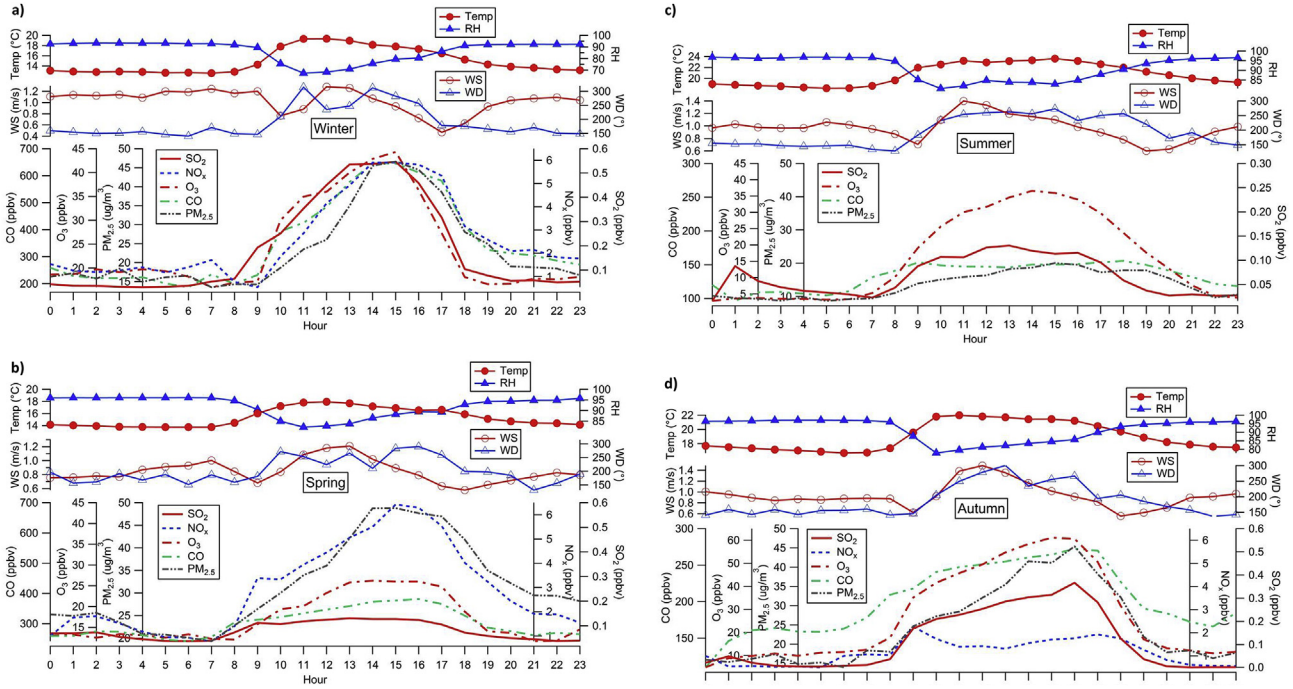

Fig. 3. a–d. Diurnal profiles of $PM_{2.5}$ (μg/m^3) (measured by TEOM), SO_2, NO_x, O_3 and CO (ppbv) in a) winter, b) spring, c) summer, and d) autumn are plotted. Meteorological data including temperature (Temp) (°C), wind speed (WS) (m/s), wind direction (WD)(°) and relative humidity (RH)(%) are also presented. No data is available for NO_x during summer due to malfunction of the equipment.

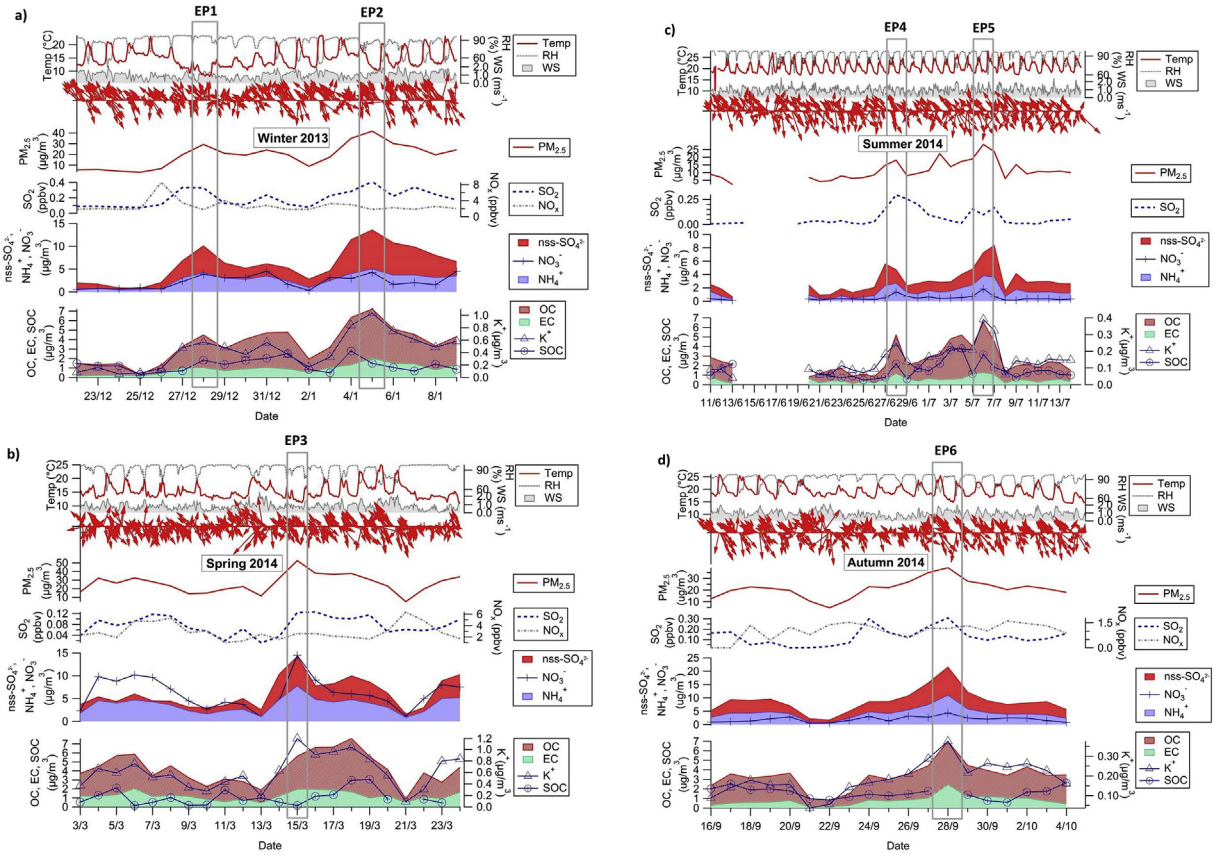

Fig. 4. a–d. Temporal variations of $PM_{2.5}$, nss-SO_4^{2-}, NO_3^-, NH_4^+, K^+, OC, EC and SOC (μg/m^3) and gases, SO_2 and NO_x (ppbv) (24-hr average) in a) winter, b) spring, c) summer and d) autumn. Hourly average of temperature (Temp) (°C), wind speed (WS) (m/s), wind direction (as shown in red arrow) and relative humidity (RH) (%) are presented. The box highlights the episode days with high concentrations of $PM_{2.5}$, ions (nss-SO_4^{2-}, NO_3^-, NH_4^+), OC and EC. NO_x data is not available during summer due to malfunction of equipment. (For interpretation of the references to colour in this figure legend, the reader is referred to the Web version of this article.)

photo-oxidation of both biogenic and anthropogenic VOCs (locally emitted from traffic and/or transported from nearby industrial sources) due to the high solar radiation in summertime.

Besides the effective transport of the local mountain-valley circulations, the long-range transport of pollutants from regional sources has significantly impacted the study site. Back-trajectories were plotted for all sampling days in different seasons (see Section S8 and Figs. S7a–d), indicating that air masses from eastern and northern China in winter (winter monsoon) were likely contributed to the higher pollutant concentrations (i.e., $PM_{2.5}$, nss-SO_4^{2-}, NO_3^-, K^+, EC and OC) in winter (Fig. S7a), as the impacts of East Asian winter monsoon on the enhancement of aerosol mass concentration and its constituents in northern and central Taiwan has been well recorded (Hsu et al., 2010; Chen et al., 2015; Chou et al., 2017). Air masses from southern and eastern China, and southeast Asian region (e.g. Vietnam and Laos) has impacted the pollutant concentrations (especially on carbonaceous species and K^+ since biomass burning in Indochina and southeast were known to severely impacted the western Pacific region) during springtime (late February to April) (Huang et al., 2016, Dong et al., 2018) (Fig. S7b).

3.4. Chemical associations

The equivalent concentration (in neq/m^3) was calculated to facilitate the stoichiometric analysis of individual or groups of cations and anions to access the correlation between them. There was a strong correlation between total cations and total anions measured (see Table 1), showing balance of charges and validity of the data (Fig. S5a). The correlation between NH_4^+ and nss-SO_4^{2-} was strong ($r = 0.9461$, $p < 0.001$), with $[NH_4^+]/[\text{nss-}SO_4^{2-}]$ ratio (1.2) higher than unity (Fig. S5b). $[NH_4^+ + \text{nss-}Ca^{+} + Mg^{2+}]$ versus $[\text{nss-}SO_4^{2-}]$ was plotted (Fig. S5c) and the ratio is similar to that of $[NH_4^+]/[\text{nss-}SO_4^{2-}]$, indicating that the contribution of nss-Ca^+ and Mg^{2+} from crustal materials was minimun. On the plot of $[NH_4^+]$ versus $[\text{nss-}SO_4^{2-} + NO_3^-]$, most of samples fall on unity (Fig. S5d), suggesting that most of the $PM_{2.5}$ consists of secondary inorganic aerosols (SIA) of ammonium sulfate ($(NH_4)_2SO_4$) and ammonium nitrate (NH_4NO_3), from the neutralization of sulfuric and nitric acids with ammonia. The neutralization factor (NF) has been used to evaluate the neutralization capacity of cations (e.g. nss-Ca^+, Mg^{2+}, NH_4^+ and K^+) with major acidic ions (SO_4^{2-} and NO_3^-) (see Section S6 and Table S3). The NF of NH_4^+ was the highest ranged from 0.89 to 1.08, indicating that the $PM_{2.5}$ at Xitou is indeed ammonium-rich.

Potassium ion was found to be moderately correlated with NO_3^- ($r = 0.8090$, $p < 0.001$), while there was relatively poor correlation ($r = 0.5837$, $p < 0.001$) between K^+ and nss-SO_4^{2-} (Figs. S5e–f). However, when the samples were differentiated into different seasons, a significant correlation could be found between K^+ and nss-SO_4^{2-} for all seasons (Fig. S6). As depicted in Fig. S6, K^+ was significantly correlated with nss-SO_4^{2-} in different seasons (although higher K^+/nss-SO_4^{2-} were found in winter and autumn, as indicated by higher slopes). In fact, NF of K^+ was higher than that of nss-Ca^+ and Mg^{2+} (see Table S3), indicating that K^+ contributes significant portion to the neutralization of acidic ions, and its concentration

was added in addition to NH_4^+ to balance the group of nss-SO_4^{2-} and NO_3^-. The slope has increased from 0.94 in the plot [NH_4^+] versus [nss-SO_4^{2-} + NO_3^-] to 0.99 in the plot [NH_4^++K^+] versus [nss-SO_4^{2-} + NO_3^-] (Figs. S5d and S5g). The results implied that K_2SO_4 and/or KNO_3 were significantly present which could be attributed to combustion activities from biomass burning (wood and grass) in suburban towns and villages and/or municipal waste incineration around the site in all seasons. The contribution of biomass burning was shown to be very significant at the study site (the temporal variation of K^+ was in fact similar to that of $PM_{2.5}$, OC and EC as shown by high Pearson correlation in Table S4) and this is further discussed in Section 3.5.

3.5. Biomass burning contribution of K^+

K^+_{excess} has been calculated which represents potassium ion contributed by biomass burning in excess of those from natural sources such as soil dust and sea salt (Cachier et al., 1995; Chen et al., 2014; Yao et al., 2016). The computation of K^+_{excess} was described in Section S2. The K^+_{excess} was found to be 0.35 in winter, 0.52 in spring, 0.09 in summer and 0.09 in autumn (see Table S5). K^+_{excess} larger than 0 implies the contribution of K^+ from biomass burning. Hence, although K^+ was found to be varied simultaneously with $PM_{2.5}$, OC and EC in all seasons, the contribution from biomass burning were higher during wintertime (Dec) and spring (Mar) seasons (concentration of K^+_{excess} is about 4–5 times more than that during summer and autumn). Intense straw burning activities occurred at rice farms in central Taiwan during wintertime (i.e. Yulin county contains the largest number of rice farms in Taiwan), as well as long-range transport of carbonaceous species from regional sources in winter and spring (see Figs. S7a–b and Section S8). The mass ratio of excess potassium to EC (K^+_{excess}/EC) indicates relative contributions of biomass burning and fossil-fuel combustion to carbonaceous-aerosol concentration (Cachier et al., 1995). The average K^+_{excess}/EC measured at Xitou was 0.36 in winter, 0.41 in spring, 0.13 in summer and 0.10 in autumn (Table S5). The average K^+_{excess} for all the samples (N = 77) was 0.26, which are in similar range as those obtained in Yucheng in North China Plain (0.18) and 3 cities in Sizhuan Plain of China (0.12–0.20) where significant impact of biomass burning were observed (Chen et al., 2014; Yao et al., 2016).

3.6. Secondary transformation of gaseous SO_2 and NO_2

To evaluate the degree of atmospheric conversion of SO_2 to nss-SO_4^{2-}, and NO_2 to NO_3^- in terms of oxidation and partitioning (e.g. Wang et al., 2005; Bencs et al., 2008; Gu et al., 2011; Squizzato et al., 2013), sulfur oxidation (SOR) and nitrogen oxidation ratios (NOR), which defined as SOR = nss-SO_4^{2-}/(nss-SO_4^{2-} + SO_2) and NOR=NO_3^-/(NO_3^- + NO_2) were calculated (see Table 2). It should be noted that the computed SOR and NOR include only the aerosol fraction and not gaseous oxidation products (e.g., HNO_3 and H_2SO_4) (Squizzato et al., 2013). Previous studies suggested that a SOR greater than 0.10 implied occurrences of photochemical oxidation of SO_2 in the atmosphere (Ohta and Okita, 1990). High SOR value was observed (average = 0.93 ± 0.05), inferring that most of the SO_2 was transformed to nss-SO_4^{2-} during the uphill transport. The SOR (for $PM_{2.5}$) measured in this study (0.725–0.993) is notably higher compared to that obtained in other urban sites (e.g. 0.12–0.39 in Beijing, 0.19 in Tianjin, 0.18–0.62 in Jinan and 0.22–0.62 in Italy, and 0.36–0.38 in Tanzania), as well as rural sites (e.g. 0.10–0.49 in Jinan, 0.35–0.65 in Japan, and 0.22–0.78 in Tanzania) (Wang et al., 2005; Gu et al., 2011; Chiwa, 2010; Yang et al., 2012; Mmari et al., 2013; Squizzato et al., 2013). Due to a longer residence time of SO_4^{2-} which are likely to undergo transformation during transport from distant sources, SOR in rural sites were generally higher than that in urban sites (Satsumabayashi et al., 1999; Chiwa, 2010). The formation of SO_4^{2-} is mainly attributed to the gas-phase oxidation by OH radicals followed by nucleation and condensation growth, or heterogeneous uptake of SO_2 on pre-existing particles or fog/cloud droplets followed by oxidation by O_3, H_2O_2, or O_2 catalyzed by Fe (III) and Mn(II) (Calvert et al., 1985; Berresheim and Jaeschke, 1986; Mather et al., 2003; Seinfeld and Pandis, 2006). It is known that the gas-phase reaction of SO_2 to sulfate is closely associated with temperature (Seinfeld and Pandis, 2006), and increasing evidences showed that sulfate is predominantly formed through heterogeneous reaction processes in polluted urban environment which is affected by RH (Buzcu et al., 2006; Wang et al., 2012; Sun et al., 2006, 2013; Zhao et al., 2013). Xitou Forest is located in central Taiwan with a humid subtropical climate and is characterized with high RH (average RH of 87.1–92.1%) for different seasons, and hence the aqueous-phase oxidation of SO_2 could be strongly enhanced and attributed to the exceptionally high sulfur oxidation state. NOR observed in this study (average = 0.39 ± 0.20; ranged between 0.020 and 0.860) was also found to be higher than that observed in other urban sites (e.g. 0.04–0.08 in Beijing, 0.19 in Tianjin and 0.01–0.08 in Italy and 0.015–0.022 in Tanzania), and rural sites (e.g. 0.034–0.067 in Tanzania) (Wang et al., 2005; Gu et al., 2011; Mmari et al., 2013; Squizzato et al., 2013). It should be noted that a significant fraction of the oxidation products of NO_2 could exist in gas phase, and the true value of NOR should be even higher than that presented here. This effect is particularly obvious in the

Table 2
Sulfate and nitrate oxidation ratios, nss-SO_4^{2-}, NO_3^- and SO_2 and NO_2 concentrations at Xitou.

		SOR	NOR	nss-SO_4^{2-} μg/m^3	SO_2 ppbv	NO_3^- μg/m^3	NO_2 ppbv
Winter	Average	0.878	0.279	6.06	0.19	2.16	2.44
n = 19	σ	0.054	0.150	3.83	0.11	1.43	1.35
Spring	Average	0.952	0.481	6.11	0.08	6.19	2.91
n = 22	σ	0.026	0.183	3.25	0.03	3.32	1.36
Summer	Average	0.932	-[a]	3.01	0.06	0.48	-[a]
n = 28	σ	0.063	-[a]	1.81	0.08	0.37	-[a]
Autumn	Average	0.949	0.383	8.68	0.12	1.97	3.46
N = 19	σ	0.026	0.209	4.48	0.08	1.03	6.61
Total	Average	0.929	0.386[b]	5.67	0.11	2.59	3.19[b]
n = 88	σ	0.054	0.197[b]	3.88	0.09	2.86	3.69[b]

[a] No NO_2 data was available due to malfunction of the equipment.
[b] Total number of samples for calculation of NOR and NO_2 is 60.

summertime. The enhanced conversion of NO_2 could either attribute to gas phase oxidation of NO_2 during daytime and/or heterogeneous reaction of N_2O_5 during nighttime (Ravishankara, 1997; Seinfeld and Pandis, 2006; Wagner et al., 2008; Pathak et al., 2009). Nevertheless, aged sulfate and nitrate could be transported during the long-range transport from surrounding regional sources (see Figs. S7a–d). The exact formation pathways of sulfate and nitrate necessitate further study to explain the high SOR and NOR observed in this study.

4. Conclusions

Four seasonal measurement campaigns on $PM_{2.5}$ concentration and composition were conducted from 2013 to 2014 at Xitou, a high-elevated subtropical forested area in Taiwan surrounded by a complex topography with highly mountainous areas (up to 3000 m) in the east, south and west, and an urban/industrialized area in the northwest. Distinct seasonal variations were observed in the concentration and composition of $PM_{2.5}$. High NO_3^- concentration and NOR observed in spring season indicated that significant amount of nitrogen oxides was converted to NO_3^-. The seasonally specific source of nitrate in springtime could due to fertilization at high-elevated tea plantations and farmlands in the surrounding areas. OC and EC concentrations in spring were also the highest among the seasons, but the highest SOC fraction, constituting 13.2% of $PM_{2.5}$ mass, was observed in summertime, evidencing the significance of photo-oxidation reactions in SOC formation due to the enhanced solar radiation. A close correlation between K^+ with OC as well as EC was depicted in all seasons, indicating substantial influences due to the biomass burning activities in the suburban towns and villages and/or municipal waste incineration around the site. The transport of pollutants from the urban sources was found to be dependent on the mountain-valley circulations, where polluted air mass was uplifted and transported by the northwesterly winds (valley breezes) during the daytime, and relatively clean air mass was transported by the southeasterly winds (mountain breezes) during the nighttime, as well as the long-range transport. Notably high SOR and NOR were observed at Xitou, which indicated the significant formation of secondary aerosol species (i.e. SO_4^{2-} and NO_3^-) from their gaseous precursors, likely due to the enhanced aqueous-phase and/or heterogeneous reactions under the exceptionally high RH condition in the subtropical forested area. This study has demonstrated the significant impacts of anthropogenic pollutants from an urban metropolis and its surrounding areas, and long-range transport from regional sources on air quality of a high-elevated forest, yielding significant amount of secondary aerosols, mostly in the form of sulfate, followed by nitrate and other secondary organic products.

Acknowledgements

The authors gratefully acknowledge the logistic supports from the Experimental Forest, National Taiwan University, and the financial supports from the Academia Sinica and the Ministry of Science and Technology of Taiwan through grants 105-2111-M-001-005-MY3, 104-2119-M-001-010 and 103-2111-M-001-003. The authors are thankful to Ms. Fu-Hui Shen and Ms. Ching-Chun Chen for their technical assistance in ED-XRF analysis.

Appendix A. Supplementary data

Supplementary data to this article can be found online at https://doi.org/10.1016/j.envpol.2018.11.033.

References

Anderson, J.O., Thundiyil, J.G., Stolbach, A., 2012. Clearing the air: a review of the effects of particulate matter air pollution on human health. J. Med. Toxicol. 8, 166–175.

Andreae, M.O., 1983. Soot carbon and excess fine potassium: long-range transport of combustion-derived aerosols. Science 220, 1148–1151.

Bencs, L., Ravindra, K., de Hoog, J., Rasoazanany, E.O., Deutsch, F., Bleux, N., Berghmans, P., Roekens, E., Krata, A., Van Grieken, R., 2008. Mass and ionic composition of atmospheric fine particles over Belgium and their relation with gaseous air pollutant. J. Environ. Monit. 10, 1148–1157.

Berresheim, H., Jaeschke, W., 1986. Study of metal aerosol systems as a sink for atmospheric SO_2. J. Atmos. Chem. 4, 311–334.

Buzcu, B., Yue, Z.W., Fraser, M.P., Nopmongcol, U., Allen, D.T., 2006. Secondary particle formation and evidence of heterogeneous chemistry during a wood smoke episode in Texas. J. Geophys. Research 111, D10S13. https://doi.org/10.1029/2005JD006143.

Cachier, H., Liousse, C., Buat-Menard, P., Gaudichet, A., 1995. Particulate content of savanna fire emissions. J. Atmos. Chem. 22, 123–148.

Calvert, J., Lazrus, A., Kok, G., Heikes, B., Walega, J., Lind, J., Cantrell, C., 1985. Chemical mechanisms of acid generation in the troposphere. Nature 317, 27–35. https://doi.org/10.1038/317027a0.

Cao, J.-J., Shen, Z.-X., Chow, J.C., Watson, J.G., Lee, S.-C., Tie, X.-X., Ho, K.-F., Wang, G.-H., Han, Y.-M., 2012. Winter and summer $PM_{2.5}$ chemical compositions in fourteen Chinese cities. J. Air Waste Manag. Assoc. 62 (10), 1214–1226.

Carrico, C.M., Bergin, M.H., Shrestha, A.B., Dibb, J.E., Gomes, L., Harris, J.M., 2003. The importance of carbon and mineral dust to seasonal aerosol properties in the Nepal Himalaya. Atmos. Environ. 37, 2811–2824.

Chang, S.-C., Chou, C.C.-K., Chan, C.-C., Lee, C.-T., 2010. Temporal characteristics from continuous measurements of $PM_{2.5}$ and speciation at the Taipei Aerosol Supersite from 2002-2008. Atmos. Environ. 44, 1088–1096.

Charlson, R.J., Schwartz, S.E., Hales, J.M., Cess, R.D., Coakley Jr., J.A., Hansen, J.E., Hofmann, D.J., 1992. Climate forcing by anthropogenic aerosols. Science 255, 423–430. https://doi.org/10.1126/science.255.5043.423.

Chen, Y., Xie, S.D., Luo, B., Zhai, C.Z., 2014. Characteristics and origins of carbonaceous aerosol in the Sichuan Basin, China. Atmos. Environ. 94, 215–223.

Chen, Y.-C., Hsu, C.-Y., Lin, S.-L., Chang-Chien, G.-P., Chen, M.-J., Fang, G.-C., Chiang, H.-C., 2015. Characteristics of concentrations and metal compositions for $PM_{2.5}$ and $PM_{2.5-10}$ in Yunlin County, Taiwan during air quality deterioration. Aerosol Air Qual. Res. 15, 2571–2583.

Cheng, M.-T., Horng, C.-L., Su, Y.-R., Lin, L.-K., Lin, Y.-C., Chou, C.C.-K., 2009. Particulate matter characteristics during agricultural waste burning in Taichung City, Taiwan. J. Hazard Mater. 165 (1–3), 187–192.

Chiwa, M., 2010. Characteristics of atmospheric nitrogen and sulfur containing compouds in an inland suburban-forested site in northern Kyushu, western Japan. Atmos. Res. 96, 531–543.

Chou, C.C.-K., Lee, C.-T., Chen, W.-N., Chang, S.-Y., Chen, T.-K., Lin, C.-Y., Chen, J.-P., 2007. Lidar observations of the diurnal variations in the depth of urban mixing layer: a case study on the air quality deterioration in Taipei, Taiwan. Sci. Total Environ. 374 (1), 156–166.

Chou, C.C.-K., Lee, C.T., Cheng, M.T., Yuan, C.S., Chen, S.J., Wu, Y.L., Hsu, W.C., Lung, S.C., Hsu, S.C., Lin, C.Y., Liu, S.C., 2010. Seasonal variation and spatial distribution of carbonaceous aerosols in Taiwan. Atmos. Chem. Phys. 10, 9563–9578.

Chou, C.C.-K., Hsu, W.-C., Chang, S.-Y., Chen, W.-N., Chen, M.-J., Huang, W.-R., Huang, S.-H., Tsai, C.-Y., Chang, S.-C., Lee, C.-T., Liu, S.-C., 2017. Seasonality of the mass concentration and chemical composition of aerosols around an urbanized basin in East Asia. J. Geophys. Research – Atmos. 122, 2026–2042. https://doi.org/10.1002/2016JD025728.

Chow, J.C., Watson, J.G., Crow, D., Lowenthal, D.H., Merrifield, T., 2001. Comparison of IMPROVE and NIOSH carbon measurements. Aerosol Sci. Technol. 34, 23–34.

Chuang, M.-T., Lee, C.-T., Chou, C.C.-K., Lin, N.-H., Sheu, G.-R., Wang, J.-L., Chang, S.-C., Wang, S.-H., Chi, K.H., Young, C.-Y., Huang, H., Chen, H.-W., Weng, G.-H., Lai, S.-Y., Hsu, S.-P., Chang, Y.-J., Chang, J.-H., Wu, X.-C., 2014. Carbonaceous aerosols in the air masses transported from Indochina to Taiwan: long-term observation at Mt. Lulin. Atmos. Environ. 89, 507–516.

Collins, W.D., Rasch, P.J., Eaton, B.E., Fillmore, D.W., Kiehl, J.T., Beck, C.T., Zender, C.S., 2002. Simulation of aerosol distributions and radiative forcing for INDOEX: regional climate impacts. J. Geophys. Research 107 (D19), 8028. https://doi.org/10.1029/2000JD000032.

Dan, M., Zhuang, G.S., Li, X.X., Tao, H.R., Zhuang, Y.H., 2004. The characteristics of carbonaceous species and their sources in $PM_{2.5}$ in Beijing. Atmos. Environ. 38, 3443–3452.

Day, D.A., Liu, S., Russell, L.M., Ziemann, P.J., 2010. Organonitrate group concentrations in submicron particles with high nitrate and organic fractions in coastal southern California. Atmos. Environ. 44 (16), 1970–1979.

Dong, X., Fu, J.S., Huang, K., Lin, N.-H., Wang, S.-H., Yang, C.-E., 2018. Analysis of the co-existence of long-range transport biomass burning and dust in the subtropical west Pacific region. Sci. Rep. 8, 8962. https://doi.org/10.1038/s41598-018-27129-2.

Gao, X., Xue, L., Wang, X., Wang, T., Yuan, C., Gao, R., Zhou, Y., Nie, W., Zhang, Q., Wang, W., 2012. Aerosol ionic components at Mt. Heng in central southern China: abundances, size distribution, and impacts of long-range transport. Sci. Total Environ. 433, 498–506.

Gu, J., Bai, Z., Li, W., Wu, L., Liu, A., Dong, H., Xie, Y., 2011. Chemical composition of $PM_{2.5}$ during winter in Tianjin, China. Particuology 9, 215–221.

Hsu, S.C., Liu, S.C., Tsai, F., Engling, G., Lin, I.I., Chou, C.K.C., Kao, S.J., Lung, S.C.C., Chan, C.Y., Lin, S.C., Huang, J.C., Chi, K.H., Chen, W.N., Lin, F.J., Huang, C.H., Kuo, C.L., Wu, T.C., Huang, Y.T., 2010. High wintertime particulate matter pollution over an offshore island (Kinmen) off southeastern China: an overview. J. Geophys. Research 115, D17309. https://doi.org/10.1029/2009JD013641.

Hsu, C.-Y., Chiang, H.-C., Chen, M.-J., Chuang, C.-Y., Tsen, C.-M., Fang, G.-C., Tsai, Y.-I., Chen, N.-T., Lin, T.-Y., Lin, S.-L., Chen, Y.-C., 2017. Ambient PM2.5 in the residential area near industrial complexes: Spatiotemporal variation, source apportionment, and health impact. Sci. Total Environ. 590-591, 204–214.

Huang, W.-R., Wang, S.-H., Yen, M.-C., Lin, N.-H., Promchote, P., 2016. Interannual variation of springtime biomass burning in Indochina: regional differences, associated atmospheric dynamical changes, and downwind impacts. J. Geophys. Res. Atmos. 121.

Kerns, B.W.J., Chen, Y.-L., 2010. The diurnal cycle of winds, rain, and clouds over Taiwan during the Mei-Yu, summer, and autumn rainfall regimes. Mon. Weather Rev. 138, 497–516.

Kido, M., Osada, K., Matsunaga, K., Iwasaka, Y., 2001a. Temporal change in ammonium/sulfate ratios for free tropospheric aerosols from early winter to spring at high elevation site in the Japanese Alps. J. Environ. Chem. 11, 33–41.

Kido, M., Osada, K., Matsunaga, K., Iwasaka, Y., 2001b. Diurnal variation of ionic aerosol species and water-soluble gas concentrations at a high-elevation site in the Japanese Alps. J. Geophys. Research 106 (D15), 17335–17345.

Kim, K.H., Kabir, E., Kabir, S., 2015a. A review on the human health impact of airborne particulate matter. Environ. Int. 74, 136–143.

Kim, P.S., Jacob, D.J., Fisher, J.A., Travis, K., Yu, K., Zhu, L., Yantosca, R.M., Sulprizio, M.P., Jimenez, J.L., Campuzano-Jost, P., Froyd, K.D., Liao, J., Hair, J.W., Fenn, M.A., Butler, C.F., Wagner, N.L., Gordon, T.D., Welti, A., Wennberg, P.O., Crounse, J.D., St Clair, J.M., Teng, A.P., Millet, D.B., Schwarz, J.P., Markovic, M.Z., Perring, A.E., 2015b. Sources, seasonality, and trends of southeast US aerosol: an integrated analysis of surface, aircraft, and satellite observations with the GEOS-Chem chemical transport model. Atmos. Chem. Phys. 15, 10411–10433.

Kuo, C.-Y., Cheng, F.-C., Chang, S.-Y., Lin, C.-Y., Chou, C.C.K., Chou, C.-H., Lin, Y.-R., 2013. Analysis of the major factors affecting the visibility degradation in two stations. J. Air Waste Manag. Assoc. 63 (4), 433–441.

Lee, C.-T., Chuang, M.-T., Lin, N.-H., Wang, J.-L., Sheu, G.-R., Chang, S.-C., Wang, S.-H., Huang, H., Chen, H.-W., Liu, Y.-L., Weng, G.-H., Lai, H.-Y., Hsu, S.P., 2011. The enhancement of $PM_{2.5}$ mass and water-soluble ions of biosmoke transported from Southeast Asia over the Mountain Lulin site in Taiwan. Atmos. Environ. 45, 5784–5794.

Lee, C.-G., Yuan, C.-S., Chang, J.-C., Yuan, C., 2005. Effects of aerosol species on atmospheric visibility in Kaohsiung city, Taiwan. J. Air Waste Manag. Assoc. 55, 1031–1041.

Lee, T., Yu, X.-Y., Kreidenweis, S.M., Malm, W.C., Collett, J.L., 2008. Semi-continuous measurement of $PM_{2.5}$ ionic composition at several rural locations in the United States. Atmos. Environ. 42, 6655–6669.

Lelieveld, J., Crutzen, P.J., Ramanathan, V., Andreae, M.O., Brenninkmeijer, C.A.M., Campos, T., Cass, G.R., Dickerson, R.R., Fischer, H., de Gouw, J.A., Hansel, A., Jefferson, A., Kley, D., de Laat, A.T.J., Lal, S., Lawrence, M.G., Lobert, J.M., Mayol-Bracero, O.L., Mitra, A.P., Novakow, T., Oltmans, S.J., Prather, K.A., Reiner, T., Rodhe, H., Scheeren, H.C., Sikka, D., Williams, J., 2001. The indian ocean experiment: widespread air pollution from south and southeast Asia. Science 291, 1031–1036.

Lelieveld, J., Evans, J.S., Fnais, M., Giannadaki, D., Pozzer, A., 2015. The contribution of outdoor air pollution sources to premature mortality on a global scale. Nature 525 (7569), 367–371.

Li, L., Wang, W., Feng, J., Zhang, D., Li, H., Gu, Z., Wang, B., Sheng, G., Fu, J., 2010. Composition, source, mass closure of $PM_{2.5}$ aerosols for four forests in eastern China. J. Environ. Sci. 22 (3), 405–412.

Li, P.-H., Wang, Y., Li, T., Sun, L., Yi, X., Guo, L.-Q., Su, R.-H., 2015. Characterization of carbonaceous aerosols at Mount Lu in South China: implication for secondary organic carbon formation and long-range transport. Environ. Sci. Pollut. Res. 22, 14189–14199.

Li, T.-C., Yuan, C.-S., Huang, H.-C., Lee, C.-L., Wu, S.-P., Tong, C., 2016. Inter-comparison of seasonal variation, chemical characteristics, and source identification of atmospheric fine particles on both sides of the Taiwan Strait. Sci. Rep. 6, 22956. https://doi.org/10.1038/srep22956.

Lin, C.-Y., Chen, W.-N., Liu, S.C., Liou, Y.A., Liu, G.R., Lin, T.H., 2008. Numerical study of the impact of urbanization on the precipitation over Taiwan. Atmos. Environ. 42, 2934–2947.

Ma, X., Yu, F., 2015. Seasonal and spatial variations of global aerosol optical depth: multi-year modeling with GEOS-Chem-APM and comparisons with multiple-platform observations. Tellus B 67, 25115.

Mather, T.A., Allen, A.G., Oppenheimer, C., Pyle, D.M., McGonigle, A.J.S., 2003. Size-resolved characterization of soluble ions in the particles in the tropospheric plume of Masaya Volcano, Nicaragua: origins and plume processing. J. Atmos. Chem. 46, 207–237.

Mmari, A.G., Potgieter-Vermaak, S.S., Bencs, L., McCrindle, R.I., van Grieken, R., 2013. Elemental and ionic components of atmospheric aerosols and associated gaseous pollutants in and near Dar es Salaam, Tanzania. Atmos. Environ. 77, 51–61.

Myhre, G., 2009. Consistency between satellite-derived and modeled estimates of the direct aerosol effect. Science 35, 187–190. https://doi.org/10.1126/science.1174461.

Ohta, S., Okita, T., 1990. A chemical characterization of atmospheric aerosol in Sapporo, Atmos. Environ. Times 24A, 815–822.

Pathak, R.K., Wu, W.S., Wang, T., 2009. Summertime $PM_{2.5}$ ionic species in four major cities of China: nitrate formation in an ammonia-deficient atmosphere. Atmos. Chem. Phys. 9, 1711–1722.

Perring, A.E., Wisthaler, A., Graus, M., Wooldridge, P.J., Lockwood, A.L., Mielke, L.H., Shepson, P.B., Hansel, A., Cohen, R.C., 2009. A product study of the isoprene+NO_3 reaction. Atmos. Chem. Phys. 9, 4945–4956.

Ravishankara, 1997. Heterogeneous and multiphase chemistry in the troposphere. Science 276, 1058–1065.

Rengarajan, R., Sarin, M.M., Sudheer, A.K., 2007. Carbonaceous and inorganic species in atmospheric aerosols during wintertime over urban and high-altitude sites in North India. J. Geophys. Research 112, D21307. https://doi.org/10.1029/2006JD008150.

RTI, 2009. Standard Operating Procedure for the X-ray Fluorescence Analysis of Particulate Matter Deposits on Teflon Filters. Environmental and Industrial Measurements Division, Research Triangle Park, North Carolina.

Satake, S., Uno, I., Takemura, T., Carmichael, G.R., Tang, Y., Streets, D., Sugimoto, N., Shimizu, A., Uematsu, M., Han, J.-S., Ohta, S., 2004. Characteristics of Asian aerosol transport simulated with a regional-scale chemical transport model during the ACE-Asia observation. J. Geophys. Research 109, D19S22. https://doi.org/10.1029/2003JD003997.

Satsumabayashi, H., Sasaki, K., Katsuno, T., Shikano, M., Ohta, M., Nishizawa, H., Murano, K., Murai, H., Hatakeyama, S., Ueda, H., 1999. Behavior of airborne acidic and oxidative components in autumn and early spring in the central mountainous area of Japan. J.of Japan Soc. for Atmos. Env. 34, 219–236 (in Japanese with English summary).

Seinfeld, J.H., Pandis, S.N., 2006. Atmospheric Chemistry and Physics: from Air Pollution to Climate Change. John Wiley and Sons, Inc., New York.

Simon, S., Klemm, O., El-Madany, T., Walk, J., Amelung, K., Lin, P.-H., Chang, S.-C., Lin, N.-H., Engling, G., Hsu, S.-C., Wey, T.-H., Wang, Y.-N., Lee, Y.-C., 2016. Chemical composition of fog water at four sites in Taiwan. Aerosol Air Qual. Res. 16, 618–631.

Solomon, S., Qin, D., Manning, M., Chen, Z., Marquis, M., Averyt, K.B., Tignor, M., Miller, H.L. (Eds.), 2007. IPCC, 2007: the Physical Science Basis. Contribution of Working Group I to the Fourth Assessment Report of the Intergovernmental Panel on Climate Change. Cambridge University Press, Cambridge, U.K., and New York.

Squizzato, S., Masiol, M., Brunelli, A., Pistollato, S., Tarabotti, E., Rampazzo, G., Pavoni, B., 2013. Factors determining the formation of secondary inorganic aerosol: a case study in the Po Valley (Italy). Atmos. Chem. Phys. 13, 1927–1939.

Sun, Y., Zhuang, G., Tang, A., Wang, Y., An, Z., 2006. Chemical characteristics of PM2.5 and PM10 in haze-fog episodes in Beijing. Environ. Sci. Technol. 40, 3148–3155.

Sun, Y.L., Wang, Z.F., Fu, P.Q., Yang, T., Jiang, Q., Dong, H.B., Li, J., Jia, J.J., 2013. Aerosol composition, sources and processes during wintertime in Beijing, China. Atmos. Chem. Phys. 13, 4577–4592.

Tian, M., Wang, H., Chen, Y., Yang, F., Zhang, X., Zou, Q., Zhang, R., Ma, Y., He, K., 2016. Characteristics of aerosol pollution during heavy haze events in Suzhou, China. Atmos. Chem. Phys. 16, 7357–7371.

Tsigaridis, K., Daskalakis, N., Kanakidou, M., Adams, P.J., Artaxo, P., Bahadur, R., Balkanski, Y., Bauer, S.E., Bellouin, N., Benedetti, A., Bergman, T., Berntsen, T.K., Beukes, J.P., Bian, H., Carslaw, K.S., Chin, M., Curci, G., Diehl, T., Easter, R.C., Ghan, S.J., Gong, S.L., Hodzic, A., Hoyle, C.R., Iversen, T., Jathar, S., Jimenez, J.L., Kaiser, J.W., Kirkevåg, A., Koch, D., Kokkola, H., Lee, Y.H., Lin, G., Liu, X., Luo, G., Ma, X., Mann, G.W., Mihalopoulos, N., Morcrette, J.-J., Müller, J.-F., Myhre, G., Myriokefalitakis, S., Ng, N.L., O'Donnell, D., Penner, J.E., Pozzoli, L., Pringle, K.J., Russell, L.M., Schulz, M., Sciare, J., Seland, Ø., Shindell, D.T., Sillman, S., Skeie, R.B., Spracklen, D., Stavrakou, T., Steenrod, S.D., Takemura, T., Tiitta, P., Tilmes, S., Tost, H., van Noije, T., van Zyl, P.G., von Salzen, K., Yu, F., Wang, Z., Wang, Z., Zaveri, R.A., Zhang, H., Zhang, K., Zhang, Q., Zhang, X., 2014. The AeroCom evaluation and intercomparison of organic aerosol in a global models. Atmos. Chem. Phys. 14, 10845–10895.

Venkataraman, C., Reddy, C.K., Josson, S., Reddy, M.S., 2002. Aerosol size and chemical characteristics at Mumbai, India, during the INDOEX-IFP (1999). Atmos. Environ. 36m, 1979–1991.

Wagner, C., Hanisch, F., Holmes, N., de Coninck, H., Schuster, G., Crowley, J.N., 2008. The interaction of N_2O_5 with mineral dust: aerosol flow tube and Knudsen reactor studies. Atmos. Chem. Phys. 8, 91–109.

Wang, Y., Zhuang, G.S., Tang, A.H., Yuan, H., Sun, Y.L., Chen, S., Zheng, A.H., 2005. The ion chemistry and the source of $PM_{2.5}$ aerosol in Beijing. Atmos. Environ. 39, 3771–3784.

Wang, X., Wang, W., Yang, L., Gao, X., Nie, W., Yu, Y., Xu, P., Zhou, Y., Wang, Z., 2012. The secondary formation of inorganic aerosols in the droplet mode through heterogeneous aqueous reactions under haze conditions. Atmos. Environ. 63, 68–76.

Yang, L., Zhou, X., Wang, Z., Zhou, Y., Cheng, S., Xu, P., Gao, X., Nie, W., Wang, X., Wang, W., 2012. Airborne fine particulate pollution in Jinan, China: concentrations, chemical compositions and influence on visibility impairment. Atmos. Environ. 55, 506–514.

Yao, L., Yang, L., Chen, J., Wang, X., Xue, L., Li, W., Sui, X., Wen, L., Chi, J., Zhu, Y., Zhang, J., Xu, C., Zhu, T., Wang, W., 2016. Characteristics of carbonaceous aerosols: impact of biomass burning and secondary formation in summertime in a rural area of the North China Plain. Sci. Total Environ. 557–558, 520–530.

Yuan, S.-C., Lee, C.-G., Liu, S.-H., Chang, J.-C., Yuan, C., Yang, H.-Y., 2006. Correlation

of atmospheric visibility with chemical composition of Kaohsiung aerosols. Atmos. Res. 82, 663–679.
Zhao, X.J., Zhao, P.S., Xu, J., Meng, W., Pu, W.W., Dong, F., He, D., Shi, Q.F., 2013. Analysis of a winter regional haze event and its formation mechanism in the North China Plain. Atmos. Chem. Phys. 13, 5685–5686.
Zhou, Y., Wang, T., Gao, X., Xue, L., Wang, X., Wang, Z., Gao, J., Zhang, Q., Wang, W., 2010. Continuous observations of water-soluble ions in $PM_{2.5}$ at Mount Tai (1534 m a.s.l.) in central-eastern China. J. Atmos. Chem. 64, 107–127.
Zhou, S., Wang, Z., Gao, R., Xue, L., Yuan, C., Wang, T., Gao, X., Wang, X., Nie, W., Xu, Z., Zhang, Q., Wang, W., 2012. Formation of secondary organic carbon and long-range transport of carbonaceous aerosols at Mount Heng in South China. Atmos. Environ. 63, 203–212.